

A frequency-dependent switch from inhibition to excitation in a hippocampal unitary circuit

Masahiro Mori, Mathias H. Abegg, Beat H. Gähwiler & Urs Gerber

Brain Research Institute, University of Zurich, Winterthurerstrasse 190, CH-8057 Zurich, Switzerland

The hippocampus, a brain structure essential for memory and cognition, is classically represented as a trisynaptic excitatory circuit. Recent findings challenge this view, particularly with regard to the mossy fibre input to CA3, the second synapse in the trisynaptic pathway¹. Thus, the powerful mossy fibre input to CA3 pyramidal cells might mediate both synaptic excitation and inhibition^{2,3}. Here we show, by recording from connected cell pairs in rat entorhinal–hippocampal slice cultures, that single action potentials in a dentate granule cell evoke a net inhibitory signal in a pyramidal cell. The hyperpolarization is due to disynaptic feedforward inhibition, which overwhelms monosynaptic excitation. Interestingly, this net inhibitory synaptic response changes to an excitatory signal when the frequency of presynaptic action potentials increases. The process responsible for this switch involves the facilitation of monosynaptic excitatory transmission coupled with rapid depression of inhibitory circuits. This ability to immediately switch the polarity of synaptic responses constitutes a novel synaptic mechanism, which might be crucial to the state-dependent processing of information in associative hippocampal networks.

We studied, in hippocampal slice cultures, the unitary response in a CA3 pyramidal cell (PC) evoked by action potentials in a connected granule cell (GC). Connectivity of GCs in our slice cultures approaches that reported *in vivo*, with no evidence for sprouting^{4,5} (Fig. 1a, Supplementary Fig. 1a). In six GCs we measured a mossy fibre length of $2,008 \pm 219 \mu\text{m}$, bearing 11.8 ± 1.3 large mossy terminals with a diameter of $5.9 \pm 0.3 \mu\text{m}$, of which 70.4% gave rise to 1.6 ± 0.1 filopodial extensions in CA3 and with 13.6 ± 2.2 large mossy fibre terminals giving rise to 1.7 ± 0.1 filopodial extensions in the hilus. These values compare well with those reported for rat *in vivo*, in which mossy fibre length was $3,236 \mu\text{m}$, the number of large mossy terminals was 12.3 (range 10–18) with a diameter ranging between 4 and $10 \mu\text{m}$ with 2.3 filopodial extensions in CA3, and with 7–12 large mossy terminals in the hilus².

A single action potential in the GC induced a biphasic response in the PC consisting of a brief excitatory postsynaptic current (EPSC) reliably followed by a pronounced inhibitory postsynaptic current (IPSC) (12 of 13; Fig. 1b, Supplementary Fig. 2). The resulting charge transfer was $1,134.1 \pm 378.7 \text{ fC}$ outwards ($n = 12$), indicative of a net inhibitory synaptic response. This inhibitory response might arise through disynaptic inhibition^{2,6–8} or from the simultaneous release of glutamate and GABA from mossy fibre terminals³. To distinguish between these possibilities we blocked excitatory glutamatergic signalling with the α -amino-3-hydroxy-5-methyl-4-isoxazole propionic acid (AMPA)/kainate receptor antagonist 1,2,3,4-tetrahydro-6-nitro-2,3-dioxo-benzo[*f*]-quinoxaline-7-sulphonamide (NBQX; $10 \mu\text{M}$), which abolished both the excitatory and the inhibitory components of the response ($n = 12$; Fig. 1b). Thus, the inhibitory component reflects disynaptic feedforward or feedback inhibition. Because the unitary charge transfer in a PC evoked by a CA3 interneuron was $327.1 \pm 65.3 \text{ fC}$ ($n = 8$; five interneurons in CA3 stratum lucidum, three interneurons in stratum oriens), we estimate that at least four inter-

neurons discharged to evoke the inhibitory response in a PC after a single action potential in a GC.

Evidence for a monosynaptic excitatory connection is provided by the low variability in latency (jitter: $0.53 \pm 0.10 \text{ ms}$, $n = 7$) between the GC action potential and the postsynaptic response (Figs 1b, c and 2a) and the one-to-one transmission at high frequencies (Figs 2e, f and 3). Furthermore, evoking pharmacologically isolated *N*-methyl-D-aspartate (NMDA) receptor-mediated EPSPs, which are below firing threshold, resulted in short latency responses in 6 of 16 GC–PC pairs, which is consistent with a monosynaptic connection (Fig. 1c). The lack of a response in ten pairs reflects the absence of NMDA receptors at a significant proportion of mossy fibre synapses^{9,10}. Monosynaptic AMPA/kainate receptor-mediated EPSCs from GC–PC pairs had a response latency of $6.7 \pm 0.7 \text{ ms}$, a mean peak amplitude of $-163.0 \pm$

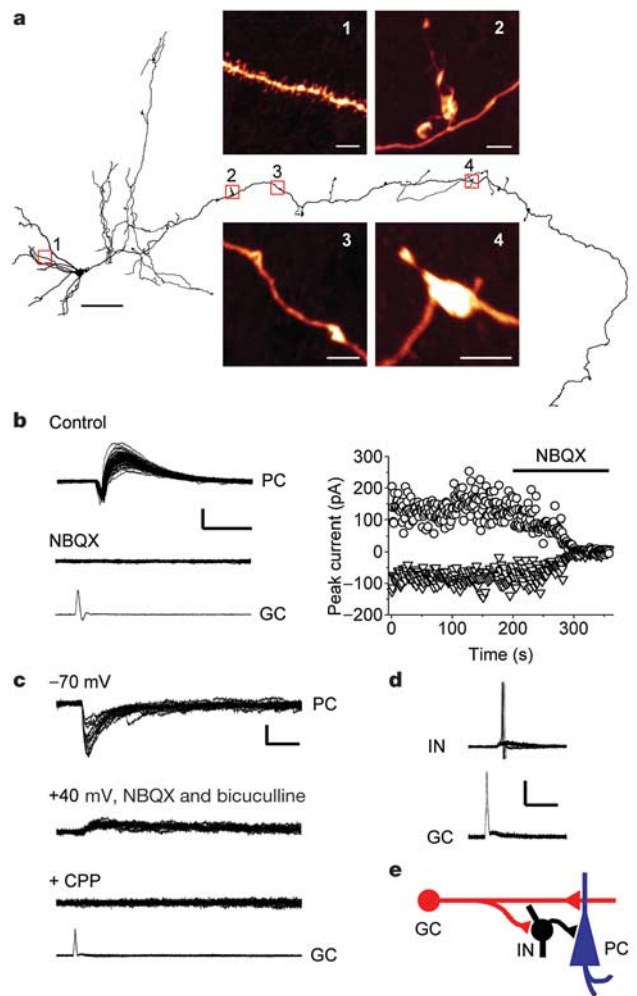


Figure 1 Unitary responses induced by single GC action potentials. **a**, A GC in slice culture (see Supplementary Fig. 1a). Boxed regions show a spiny GC dendrite (1), large mossy fibre boutons with filopodial extensions (2 and 4), and *en passant* varicosities (3). **b**, Left, single action potentials at 1 Hz in a GC (bottom) evoked biphasic currents in a PC at -70 mV (top) (see Supplementary Fig. 2), sensitive to $10 \mu\text{M}$ NBQX (middle). Right, amplitudes of EPSCs (triangles) and IPSCs (circles) plotted against time. **c**, Under suppression of IPSCs in a recorded PC (see Methods), a single action potential (1 Hz, bottom) evokes synaptic currents mediated by AMPA/kainate receptors (top), and NMDA receptors (after $20 \mu\text{M}$ NBQX and $40 \mu\text{M}$ bicuculline, upper middle), sensitive to $20 \mu\text{M}$ CPPene (lower middle). **d**, GC-evoked synaptic potentials and action potentials in an interneuron (IN) (-65 mV) (see Supplementary Fig. 1b–i). **e**, Unitary circuit for mossy fibre transmission. Vertical bars: 100 pA (PC), 100 mV (GC) (**b**); 50 pA (PC), 100 mV (GC) (**c**); 50 mV (**d**). Horizontal bars: left 100 μm , images 5 μm (**a**); 20 ms (**b–d**).

23.3 pA at -70 mV, a 20–80% rise time of 1.6 ± 0.2 ms and a decay time constant of 12.8 ± 1.1 ms ($n = 7$; Fig. 2a). The reliability of monosynaptic EPSC transmission depended strongly on the frequency with which single presynaptic action potentials were elicited (Fig. 2b) but was not modified by depolarizing the presynaptic GC by 10 mV ($83.0 \pm 6.1\%$ and $82.8 \pm 6.7\%$ for failure rates with a 3-s interval at presynaptic potentials of -70 mV and -60 mV, respectively; $P = 0.98$, $n = 4$). This result indicates that conduction failures¹¹ do not contribute significantly to the observed failures in synaptic transmission, although this mechanism cannot be ruled out. The failure rate of the first EPSP in a train decreased with repetitive trains of action potentials, presumably because of persisting residual calcium. Paired-pulse facilitation in PCs was apparent at an interspike interval shorter than 100 ms (2.54 ± 0.48 at 50 ms, $n = 5$; Fig. 2c, d). When trains of action potentials were induced in a GC, EPSC facilitation changed to a gradual depression with increasing spike frequency (Fig. 2e, f).

Activation of a single GC evoked subthreshold responses in targeted PCs, but had to have induced action potentials in the CA3 interneurons comprising the feedforward circuit (Fig. 1e). Indeed, a single action potential in a GC elicited an action potential in targeted postsynaptic interneurons ($30.3 \pm 6.1\%$ of trials at -60 mV, $n = 4$, three of five stratum lucidum interneurons; one of three stratum oriens interneurons; Fig. 1d, Supplementary Fig. 1b–i) as reported previously for hippocampal interneurons^{12,13}. Monosynaptic EPSCs from GC–interneuron pairs had a response latency of 7.0 ± 0.7 ms, a mean peak amplitude of -56.9 ± 17.7 pA

at -70 mV, a 20–80% rise time of 1.1 ± 0.3 ms, and a decay time constant of 7.3 ± 1.4 ms ($n = 5$).

GCs normally fire at low frequencies (less than 1 Hz), which can, however, increase greatly (10–40 Hz) when rats enter the place field of a GC¹⁴. To examine frequency-dependent effects on transmission, we recorded responses in a PC to trains of 15 action potentials induced in a synaptically coupled GC at frequencies ranging from 10 to 40 Hz. At 10 Hz the synaptic response to each presynaptic action potential consisted of a biphasic EPSP/IPSP sequence (Fig. 3a), with inhibition predominating as determined by calculating the area of each response (Fig. 3b). Facilitation of both EPSPs and IPSPs was observed. At firing frequencies of 20 Hz and greater, the initial facilitation of EPSPs and IPSPs was succeeded by a rapid and complete depression of the IPSP component, resulting in monophasic EPSPs (Fig. 3a–d). The progressive depression of the IPSPs was associated with a corresponding increase in duration of the EPSPs. The mean half-width of the EPSPs by the 13th to 15th action potential was 3.7 ± 0.2 ms at 10 Hz, compared with 6.8 ± 0.4 ms at 40 Hz ($n = 7$, $P < 0.05$). This frequency-dependent shift in IPSP-dominant to EPSP-dominant responses could be repeatedly reproduced by allowing a 30-s interval between trains and was unaffected by application of the GABA_B receptor antagonist CGP62349 ($3 \mu\text{M}$; $P = 0.98$, $n = 5$) or the metabotropic glutamate receptor antagonist α -methyl-4-carboxyphenylglycine (MCPG; 0.5 mM , $P = 0.96$, $n = 6$). Strong extracellular stimulation leads to chloride redistribution, reducing the driving force for inhibition¹⁵. However, when we induced trains of action potentials in a single mossy fibre, there was no apparent shift in the reversal potential for inhibition (control, -84.3 ± 1.7 mV; after 15 action potentials at 40 Hz, -85.0 ± 1.8 mV; $P = 0.77$, $n = 4$), indicating

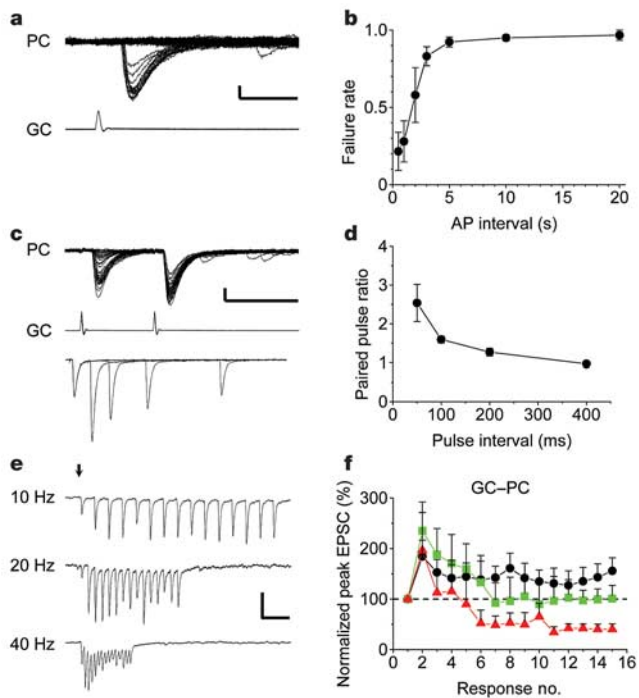


Figure 2 Frequency-dependent properties of monosynaptic mossy fibre transmission to PCs. **a**, Monosynaptic currents evoked by single GC action potentials at 0.5 Hz in a PC with inhibition blocked (-70 mV). **b**, Transmission failure decreases as action potential frequency increases ($n = 5$). **c**, Paired-pulse facilitation at an interspike interval of 50 ms at 0.5 Hz in the same cell pair as in **a**. Averaged paired-pulse responses at 50–400 ms normalized to the first response amplitude (bottom). **d**, Plot of paired-pulse ratio against pulse interval ($n = 5$). **e**, Monosynaptic currents in a PC during trains of 15 presynaptic action potentials with increasing frequencies. Traces are averages (three to five sweeps). **f**, Peak amplitude of EPSCs at 10 Hz (black), 20 Hz (green) and 40 Hz (red) plotted against evoked response number (1–15) ($n = 6$). Vertical bars: 50 pA (PC), 100 mV (GC) (**a**); 100 pA (PC), 100 mV (GC) (**c**); 100 pA (**e**). Horizontal bars: 20 ms (**a**); 50 ms (PC and GC), 200 ms (bottom) (**c**); 200 ms (**e**). Error bars, s.e.m.

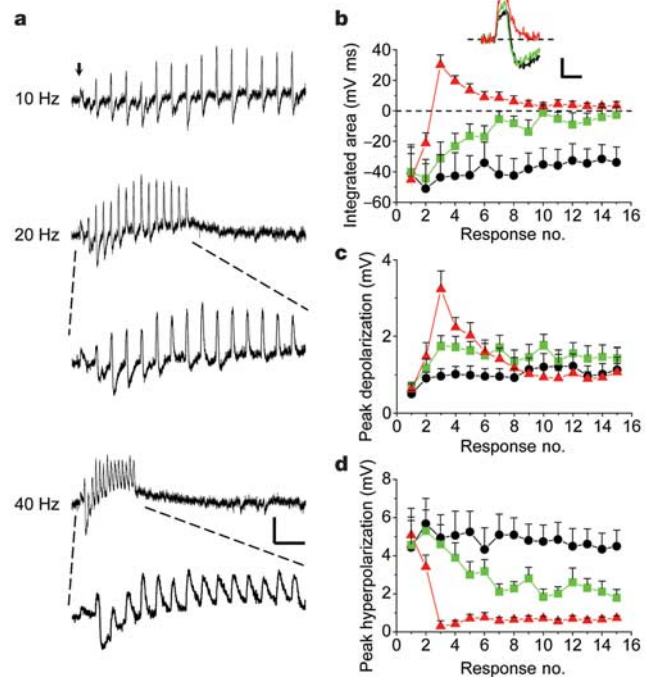


Figure 3 Switch in unitary postsynaptic potentials from inhibitory-dominant to excitatory-dominant with increasing frequency. **a**, Synaptic potentials in a PC (-70 mV) evoked by 15-action potential trains with increasing frequencies. Averages of four or five sweeps are shown. **b**, Integration of postsynaptic potentials for 20 ms after each action potential at 10 Hz (black), 20 Hz (green) and 40 Hz (red) plotted against response number (1–15) ($n = 7$). Inset, superimposition of fourth responses (**a**). **c**, **d**, Peak depolarization (**c**) and hyperpolarization (**d**) at 10 Hz (black), 20 Hz (green) and 40 Hz (red) plotted against response number ($n = 7$). Vertical bars, 3 mV (**a**); 2 mV (**b**). Horizontal bars, 200 ms; expanded traces 100 ms (20 Hz) and 50 ms (40 Hz) in **a**, 10 ms in **b**. Error bars, s.e.m.

no significant redistribution of chloride. To characterize the mechanism underlying the rapid depression of disynaptic IPSPs at high firing rates, we examined the frequency response of the two synapses involved in the feedforward inhibition of PCs (Fig. 1e). For the monosynaptic EPSCs mediating spike transmission (Fig. 1d) at the GC–interneuron synapse ($n = 5$; interneurons in stratum lucidum), EPSCs progressively facilitated at 10–20 Hz, whereas at 40 Hz the responses were depressed after the eighth action potential (Fig. 4a, b). A similar analysis at the interneuron–PC synapse ($n = 5$, interneurons in stratum lucidum) showed that GABAergic transmission was depressed rapidly at all frequencies tested (Fig. 4c, d). Thus both the GC–interneuron and interneuron–PC synapses contribute to the rapid depression of disynaptic IPSPs in response to high-frequency discharge of GCs (Fig. 4e).

These results indicate first that unitary mossy fibre transmission to PCs induces not only a monosynaptic excitatory response but also a powerful disynaptic inhibitory response resulting in net inhibition, and second that an increase in the frequency of GC firing results in a switch from an inhibitory-dominant to an excitatory-dominant postsynaptic response.

The observation that extracellular stimulation of the dentate gyrus evokes a biphasic EPSP/IPSP response in PCs¹⁶ and the demonstration of an extensive innervation of interneurons by the mossy fibres² has indicated an important role for feedforward inhibition in the modulation of activity in the CA3 area^{6–8}. Our recordings from functionally connected GC–PC pairs confirmed this hypothesis and allowed us to determine that in rat hippocampal slice cultures four or more interneurons typically contribute to this feedforward pathway. In contrast, the monosynaptic excitatory pathway generally consists of one giant synapse on a PC, containing

30–40 active zones^{2,17}. We calculated a unitary conductance of the monosynaptic glutamatergic mossy fibre response of 2.3 ± 0.3 nS ($n = 7$; Fig. 2a). This value translates to a release of 18 vesicles in response to a single presynaptic action potential, assuming a quantal conductance at room temperature of 0.13 nS (ref. 10). Under our recording conditions (34 °C), quantal size will be greater, indicating that a single action potential is likely to release at most one vesicle per active zone. At high frequencies of presynaptic action potential firing, Ca^{2+} influx enhanced by presynaptic action potential broadening¹⁸ and Ca^{2+} release from intracellular stores^{19,20} lead to a marked increase in Ca^{2+} in the terminal, which will release a large fraction of the vesicles from the readily releasable pool. However, because of the significant size of this pool (1,400) (ref. 21) it is unlikely that vesicular depletion is induced by short trains of action potentials. Thus, depression of the monosynaptic mossy fibre EPSCs (Fig. 2e, f) is probably due to other mechanisms such as postsynaptic AMPA/kainate receptor desensitization.

A unitary local neuronal network composed of one GC, a targeted PC and several interneurons will serve as a high-pass filter for incoming temporal events in which high-frequency signals will be transferred as a rate code, whereas less frequent basal events will be processed into a temporally precise code. Evidence for enhanced excitatory signals onto PCs in response to high-frequency discharge was observed in a study *in vivo* in which trains of presynaptic spikes discharged PCs more effectively²². In our study, stimulation of a single GC never evoked a suprathreshold EPSP in the PC at holding potentials between -70 and -60 mV. However, when PCs receive excitatory drive from the local associative network^{23,24}, the membrane potential will be closer to threshold, allowing unitary mossy fibre EPSPs to trigger action potentials. The frequency-dependent switch from inhibition to excitation might be important in certain forms of modulation of synaptic strength such as long-term depression and long-term potentiation^{25,26}. Thus, frequency-dependent modulation of synaptic transmission seems to be an important principle in the regulation of brain circuits^{27,28}. □

Methods

Preparation of slice cultures

Slice cultures were prepared from 6-day-old Wistar rat pups killed by decapitation in accordance with a protocol approved by the Veterinary Department of the Canton of Zurich, and maintained as described previously²⁹. In brief, 400- μ m-thick hippocampal slices including the entorhinal cortex were attached to glass coverslips with the use of clotted chicken plasma, placed in sealed test tubes with serum-containing medium, and kept in a roller-drum incubator at 36 °C for 21–28 days.

Electrophysiological recordings

Cultures were transferred to a recording chamber mounted on an upright microscope (Axioskop FS1; Zeiss) and superfused with an external solution containing 148.8 mM Na^+ , 2.7 mM K^+ , 149.2 mM Cl^- , 2.8 mM Ca^{2+} , 2.0 mM Mg^{2+} , 11.6 mM HCO_3^- , 0.4 mM $H_2PO_4^-$, 5.6 mM D-glucose and 10 mg l⁻¹ phenol red (pH 7.4). All experiments were performed at 34 °C. Recordings were obtained from PCs, interneurons in area CA3a and b, and GCs with patch pipettes (2–5 M Ω) using an Axopatch 200B amplifier (Axon Instruments). For current-clamp recording, pipettes were filled with 135 mM potassium gluconate, 5 mM KCl, 10 mM Hepes, 1 mM EGTA, 2 mM MgATP, 5 mM creatine phosphate (CrP), 0.4 mM GTP, 0.07 mM $CaCl_2$ (pH 7.2). For voltage-clamp recording, patch pipettes were filled with 121.6 mM CsF, 8.4 mM CsCl, 10 mM HEPES, 10 mM EGTA, 1 mM picrotoxin, 2 mM MgATP, 5 mM CrP, 0.4 mM GTP (pH 7.2), except that the potassium solution as above was used for the voltage-clamp recordings shown in Figs 1b and 4c. To suppress IPSCs in recorded PCs, we used a solution with fluoride as the major intracellular anion containing the GABA_A receptor antagonist picrotoxin and adjusted the equilibrium potential for chloride to correspond to the holding potential of -70 mV. Membrane potentials were corrected for liquid junction potentials. Series resistance (5–15 M Ω) was compensated but by not more than 40–90% to avoid unstable recordings, and cells were excluded if a change of more than 20% occurred. Presynaptic action potentials were evoked by injecting depolarizing current (1 ms, 1.5–2.0 nA) at 0.5 Hz unless otherwise mentioned. By recording first from a postsynaptic PC and then systematically scanning the dentate gyrus with a potassium puff electrode (140 mM K^+) to induce localized activation ('potassium puff search'), the success rate of obtaining a monosynaptic connection between a GC and a PC was increased up to 10%.

Imaging and image analysis

For staining cells, 0.1–0.2% biocytin or tetramethylrhodamine (Mioruby; Molecular Probes) was added to the pipette solutions. After experiments, slices were fixed in 4%

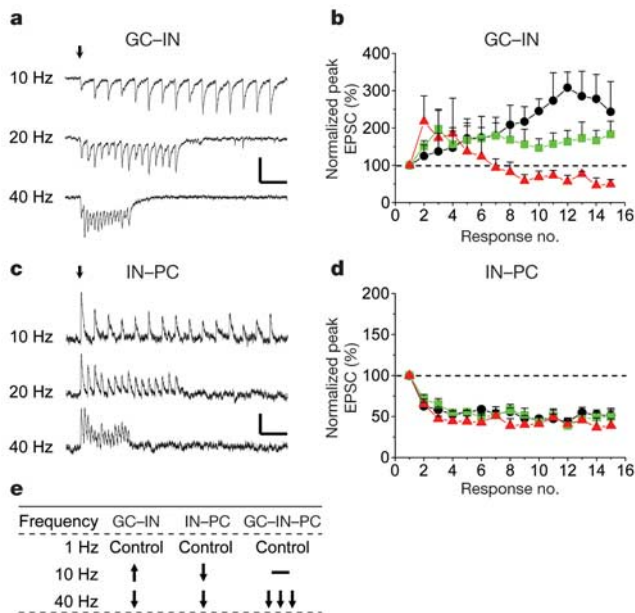


Figure 4 Depression of both GC–interneuron (GC–IN) and interneuron–PC (IN–PC) synapses at high frequency contributes to the switch from inhibitory to excitatory CA3 responses. **a**, Modulation of interneuron EPSCs with increasing action potential frequencies (-70 mV). **b**, EPSC amplitude normalized to the first EPSC at 10 Hz (black), 20 Hz (green) and 40 Hz (red) plotted against response number (1–15) in GC–interneuron pairs ($n = 5$). **c**, IPSCs at interneuron–PC synapses were depressed at 10–40 Hz. **d**, IPSC amplitude normalized to the first IPSC at 10 Hz (black), 20 Hz (green) and 40 Hz (red) plotted against response number in interneuron–PC pairs ($n = 5$). **e**, Summary of frequency-dependent modulation for GC–interneuron, interneuron–PC and GC–interneuron–PC synapses. Traces are averages of three to five sweeps. Vertical bars, 50 pA (**a**); 20 pA (**c**). Horizontal bars, 200 ms. Error bars, s.e.m.

buffered paraformaldehyde, removed from the coverslip, permeabilized for 6–12 h, incubated for 15 min in Alexa Fluor 488 streptavidin (Molecular Probes), washed again and mounted. Eight-bit image stacks were acquired on a confocal microscope (SP2; Leica) using the 40× HCXP APO (numerical aperture 1.25) oil-immersion objective. Voxel size in the xyz dimension was $0.4 \times 0.4 \times 0.5 \mu\text{m}^3$ ($0.05 \times 0.05 \times 0.5 \mu\text{m}^3$ for high resolution). Measures of axonal arborization and diameter of the large mossy terminals were performed on montages of maximal intensity projections (Supplementary Fig. 1a) using ImageJ software (National Institute of Mental Health, Bethesda, Maryland). No further filtering or image processing was used.

Drugs and chemicals

MCPG and NBQX were purchased from Tocris Cookson, and ATP, CrP, EGTA, GTP, (–)-bicuculline methochloride and 3,3′-diaminobenzidine from Sigma/Fluka. (E)-4-(3-phosphonoprop-2-enyl)piperazine-2-carboxylic acid (CPPene) and CGP62349 were kindly provided by Novartis AG.

Data acquisition and analysis

Signals were filtered at 2 or 5 kHz, digitally recorded on a computer by using CLAMPEX 7 software (Axon Instruments) and stored on tape for later analysis. The amplitude, latency and kinetics were determined as described elsewhere³⁰. To quantify the synaptic responses evoked by each action potential during a train, the peak amplitude and the area of the response were measured from the baseline directly preceding each EPSP. The standard deviation of the latencies was used to calculate the jitter. For calculation of the paired-pulse ratios, averages (including failures) were obtained. Numerical data in the text are expressed as means ± s.e.m.

Received 9 January; accepted 12 July 2004; doi:10.1038/nature02854.

1. Bischofberger, J. & Jonas, P. Two B or not two B: differential transmission at glutamatergic mossy fiber–interneuron synapses in the hippocampus. *Trends Neurosci.* **25**, 600–603 (2002).
2. Acasády, L., Kamondi, A., Sik, A., Freund, T. & Buzsáki, G. GABAergic cells are the major postsynaptic targets of mossy fibers in the rat hippocampus. *J. Neurosci.* **18**, 3386–3403 (1998).
3. Walker, M. C., Ruiz, A. & Kullmann, D. M. Monosynaptic GABAergic signaling from dentate to CA3 with a pharmacological and physiological profile typical of mossy fiber synapses. *Neuron* **29**, 703–715 (2001).
4. Zimmer, J. & Gähwiler, B. H. Cellular and connective organization of slice cultures of the rat hippocampus and fascia dentata. *J. Comp. Neurol.* **228**, 432–446 (1984).
5. Frotscher, M. & Gähwiler, B. H. Synaptic organization of intracellularly stained CA3 pyramidal neurons in slice cultures of rat hippocampus. *Neuroscience* **24**, 541–551 (1988).
6. Frotscher, M. Mossy fiber synapses on glutamate decarboxylase-immunoreactive neurons: evidence for feed-forward inhibition in the CA3 region of the hippocampus. *Exp. Brain Res.* **75**, 441–445 (1989).
7. Schwartzkroin, P. A., Scharfman, H. E. & Sloviter, R. S. Similarities in circuitry between Ammon's horn and dentate gyrus: local interactions and parallel processing. *Prog. Brain Res.* **83**, 269–286 (1990).
8. Spruston, N., Lübke, J. & Frotscher, M. Interneurons in the stratum lucidum of the rat hippocampus: an anatomical and electrophysiological characterization. *J. Comp. Neurol.* **385**, 427–440 (1997).
9. Siegel, S. J. et al. Regional, cellular, and ultrastructural distribution of N-methyl-D-aspartate receptor subunit 1 in monkey hippocampus. *Proc. Natl Acad. Sci. USA* **91**, 564–568 (1994).
10. Jonas, P., Major, G. & Sakmann, B. Quantal components of unitary EPSCs at the mossy fibre synapse on CA3 pyramidal cells of rat hippocampus. *J. Physiol. (Lond.)* **472**, 615–663 (1993).
11. Debanne, D., Guérineau, N. C., Gähwiler, B. H. & Thompson, S. M. Action-potential propagation gated by an axonal I_A -like K^+ conductance in hippocampus. *Nature* **389**, 286–289 (1997).
12. Miles, R. Synaptic excitation of inhibitory cells by single CA3 hippocampal pyramidal cells of the guinea-pig *in vitro*. *J. Physiol. (Lond.)* **428**, 61–77 (1990).
13. Debanne, D., Guérineau, N. C., Gähwiler, B. H. & Thompson, S. M. Physiology and pharmacology of unitary synaptic connections between pairs of cells in areas CA3 and CA1 of rat hippocampal slice cultures. *J. Neurophysiol.* **73**, 1282–1294 (1995).
14. Jung, M. W. & McNaughton, B. L. Spatial selectivity of unit activity in the hippocampal granular layer. *Hippocampus* **3**, 165–182 (1993).
15. Thompson, S. M. & Gähwiler, B. H. Activity-dependent disinhibition. I. Repetitive stimulation reduces IPSP driving force and conductance in the hippocampus *in vitro*. *J. Neurophysiol.* **61**, 501–511 (1989).
16. Brown, T. H. & Johnston, D. Voltage-clamp analysis of mossy fiber synaptic input to hippocampal neurons. *J. Neurophysiol.* **50**, 487–507 (1983).
17. Chicurel, M. E. & Harris, K. M. Three-dimensional analysis of the structure and composition of CA3 branched dendritic spines and their synaptic relationships with mossy fiber boutons in the rat hippocampus. *J. Comp. Neurol.* **325**, 169–182 (1992).
18. Geiger, J. R. & Jonas, P. Dynamic control of presynaptic Ca^{2+} inflow by fast-inactivating K^+ channels in hippocampal mossy fiber boutons. *Neuron* **28**, 927–939 (2000).
19. Llano, I. et al. Presynaptic calcium stores underlie large-amplitude miniature IPSCs and spontaneous calcium transients. *Nature Neurosci.* **3**, 1256–1265 (2000).
20. Liang, Y., Yuan, L. L., Johnston, D. & Gray, R. Calcium signaling at single mossy fiber presynaptic terminals in the rat hippocampus. *J. Neurophysiol.* **87**, 1132–1137 (2002).
21. Hallermann, S., Pawlu, C., Jonas, P. & Heckmann, M. A large pool of releasable vesicles in a cortical glutamatergic synapse. *Proc. Natl Acad. Sci. USA* **100**, 8975–8980 (2003).
22. Henze, D. A., Wittner, L. & Buzsáki, G. Single granule cells reliably discharge targets in the hippocampal CA3 network *in vivo*. *Nature Neurosci.* **5**, 790–795 (2002).
23. Miles, R. & Wong, R. K. Excitatory synaptic interactions between CA3 neurones in the guinea-pig hippocampus. *J. Physiol. (Lond.)* **373**, 397–418 (1986).
24. Nakazawa, K. et al. Requirement for hippocampal CA3 NMDA receptors in associative memory recall. *Science* **297**, 211–218 (2002).
25. Yeckel, M. F., Kapur, A. & Johnston, D. Multiple forms of LTP in hippocampal CA3 neurons use a common postsynaptic mechanism. *Nature Neurosci.* **2**, 625–633 (1999).
26. Kobayashi, K. & Poo, M. M. Spike train timing-dependent associative modification of hippocampal CA3 recurrent synapses by mossy fibers. *Neuron* **41**, 445–454 (2004).

27. Galarreta, M. & Hestrin, S. Frequency-dependent synaptic depression and the balance of excitation and inhibition in the neocortex. *Nature Neurosci.* **1**, 587–594 (1998).
28. Varela, J. A., Song, S., Turrigiano, G. G. & Nelson, S. B. Differential depression at excitatory and inhibitory synapses in visual cortex. *J. Neurosci.* **19**, 4293–4304 (1999).
29. Gähwiler, B. H., Thompson, S. M., McKinney, R. A., Debanne, D. & Robertson, R. T. in *Culturing Nerve Cells* 2nd edition (eds Banker, G. & Goslin, K.) 461–498 (MIT Press, Cambridge, Massachusetts, 1998).
30. Feldmeyer, D., Egger, V., Lübke, J. & Sakmann, B. Reliable synaptic connections between pairs of excitatory layer 4 neurones within a single 'barrel' of developing rat somatosensory cortex. *J. Physiol. (Lond.)* **521**, 169–190 (1999).

Supplementary Information accompanies the paper on www.nature.com/nature.

Acknowledgements We thank H. Blum, S. Giger, H. Kasper, L. Rietschin, and R. Schöb for technical assistance, and P. Streit for help in image processing. This work was funded by the Swiss National Science Foundation, the NCCR on Neural Plasticity and Repair, and the Hartmann Müller Foundation.

Competing interests statement The authors declare that they have no competing financial interests.

Correspondence and requests for materials should be addressed to M.M. (mori@hifo.unizh.ch).

Regulation of B-cell survival by BAFF-dependent PKC δ -mediated nuclear signalling

Ingrid Mecklenbräuer¹, Susan L. Kalled², Michael Leitges³, Fabienne Mackay⁴ & Alexander Tarakhovskiy¹

¹Laboratory of Lymphocyte Signaling, The Rockefeller University, New York, New York 10021, USA

²Biogen Idec, Inc., Cambridge, Massachusetts 02142, USA

³Max Planck Institute for Experimental Endocrinology, D 30625 Hannover, Germany

⁴Garvan Institute of Medical Research, St Vincent Hospital, Darlinghurst, NSW 2010, Sydney, Australia

Approximately 65% of B cells generated in human bone marrow are potentially harmful autoreactive B cells¹. Most of these cells are clonally deleted in the bone marrow, while those autoreactive B cells that escape to the periphery are anergized or perish before becoming mature B cells^{2–5}. Escape of self-reactive B cells from tolerance permits production of pathogenic auto-antibodies⁶; recent studies suggest that extended B lymphocyte survival is a cause of autoimmune disease in mice and humans⁷. Here we report a mechanism for the regulation of peripheral B-cell survival by serine/threonine protein kinase C δ (PKC δ): spontaneous death of resting B cells is regulated by nuclear localization of PKC δ that contributes to phosphorylation of histone H2B at serine 14 (S14-H2B). We show that treatment of B cells with the potent B-cell survival factor BAFF ('B-cell-activating factor belonging to the TNF family') prevents nuclear accumulation of PKC δ . Our data suggest the existence of a previously unknown BAFF-induced and PKC δ -mediated nuclear signalling pathway which regulates B-cell survival.

The increased lifespan of B cells in transgenic mice that over-express the B-cell survival factor BAFF is associated with development of lupus-like autoimmunity^{8–10}. We recently described a lupus-like autoimmune disease with defective B-cell tolerance in mice deficient for PKC δ ¹¹. In searching for the mechanism of the disease, we found that PKC δ -deficiency renders B cells BAFF-independent. Injection of a soluble BAFF receptor-Fc decoy, BAFF-R:Fc¹², in PKC δ ^{+/+} mice reduces the cellularity of the lymphoid organs (Fig. 1a, upper panel) by emptying peripheral